Sound velocities and density measurements of solid hcp-Fe and hcp-Fe–Si (9 wt.%) alloy at high pressure: Constraints on the Si abundance in the Earth's inner core

Daniele Antonangeli, Guillaume Morard, Luigi Paolasini, Gaston Garbarino, Caitlin A. Murphy, Eric Edmund, Frédéric Decremps, Guillaume Fiquet, Alexei Bosak, Mohamed Mezouar, et al.

Sound velocities and density measurements of solid hcp-Fe and hcp-Fe-Si(9wt.%) alloy at high pressure: Constraints on the Si abundance in the Earth's inner core

Daniele Antonangeli[1,*], Guillaume Morard[1], Luigi Paolasini[2], Gaston Garbarino[2], Caitlin A. Murphy[3], Eric Edmund[1], Frederic Decremps[1], Guillaume Fiquet[1], Alexei Bosak[2], Mohamed Mezouar[2], Yingwei Fei[3]

[1] Institut de Minéralogie, de Physique des Matériaux, et de Cosmochimie (IMPMC), UMR CNRS 7590, Sorbonne Universités – UPMC, Muséum National d'Histoire Naturelle, IRD UR 206, 75252 Paris, France.

[2] European Synchrotron Radiation Facility, BP 220, 38043 Grenoble Cedex, France.

[3] Geophysical Laboratory, Carnegie Institution of Washington, Washington DC 20015, USA

[*] e-mail: daniele.antonangeli@impmc.upmc.fr

Abstract

We carried out sound velocity and density measurements on solid hcp-Fe and an hcp-Fe-Si alloy with 9 wt.% Si at 300 K up to ~170 and ~ 140 GPa, respectively. The results allow us to assess the density (ρ) dependence of the compressional sound velocity (V_P) and of the shear sound velocity (V_S) for pure Fe and the Fe-Si alloy. The established V_P-ρ and V_S-ρ relations are used to address the effect of Si on the velocities in the Fe-FeSi system in the range of Si concentrations 0 to 9wt.% applicable to the Earth's core. Assuming an ideal linear mixing model, velocities vary with respect to those of pure Fe by ~ +80 m/s for V_P and ~ -80 m/s for V_S for each wt.% of Si at the inner core density of 13000 kg/m^3. The possible presence of Si in the inner core and the quantification of its amount strongly depend on anharmonic effects at high temperature and on actual core temperature.

Keywords: seismic wave velocities; iron; iron-silicon alloys; high pressure; high temperature; Earth's inner core

1. Introduction

The physical properties of iron and iron alloys at high pressure are crucial to refine the chemical composition and dynamics of the Earth's core. In this respect, density (ρ), compressional–wave (V_P) and shear-wave (V_S) sound velocities are of particular importance, as those parameters can be directly compared to seismological observations. Over the last twenty years, a great effort has been devoted to the development of experiments capable of probing sound velocity of metallic samples at high pressure, with a specific focus on iron (see *Antonangeli and Ohtani [2015]* for a recent review). Ab initio calculations have been extensively applied as well to assess material's properties at core pressures and temperatures [e.g. *Vočadlo et al., 2009; Sha and Cohen, 2010; Martorell et al., 2013*]. Yet, a consensus has not been reached, not only concerning the absolute values of velocities of solid iron at inner core conditions, but also the dependence of velocities upon pressure and temperature.

Since the seminal work of *Birch [1952]* it has been well established that light elements are alloyed to iron in the Earth's core to account for the density difference between pure Fe and seismological observations (e.g. model PREM by *Dziewonski and Anderson [1981]*). For the solid inner core, many recent experimental studies suggest silicon as one of the major candidates, based on its physical properties (density and sound velocity) and/or affinity for the metallic phase during Earth's differentiation [e.g. *Lin et al., 2003; Badro et al., 2007; Antonangeli et al., 2010; Mao et al. 2012; Siebert et al., 2013; Fischer et al., 2015; Tateno et al., 2015*]. However, different works propose different amount of Si alloyed to Fe in the inner core, ranging from ~2wt.% [*Badro et al., 2007; Antonangeli et al., 2010*] up to ~8% [*Mao et al. 2012; Fischer et al., 2015*]. One of the causes for such a discrepancy is the large pressure and temperature extrapolation necessary to compare experimental results with inner core seismological models. For instance, results based on linear extrapolations of V_P-ρ relation argued for about 2 wt% Si alloyed to Fe in the inner core [*Badro et al., 2007; Antonangeli et*

al., 2010], while a model using a power law for the V_P-ρ extrapolation proposed 8 wt% Si [*Mao et al. 2012*]. In contrast with the bulk of the experimental results, a very recent computational work on silicon alloys at inner core conditions [*Martorell et al., 2016*] suggested that both the P-wave and the S-wave velocities of any hcp-Fe-Si alloy would be too high to match the seismically observed values at inner-core density.

To shed light on this ongoing debate, we carried out sound velocity and density measurements on pure Fe and a Fe-Si alloy with 9 wt.% Si in the hexagonal close-packed structure (hcp) from ~40 GPa up to ~170 GPa, using inelastic x-ray scattering (IXS) and x-ray diffraction (XRD). IXS allows a clear identification of longitudinal aggregate excitations in polycrystalline samples [*Fiquet et al., 2001, 2009; Antonangeli et al., 2004, 2010, 2012, 2015; Badro et al., 2007; Mao et al., 2012; Ohtani et al., 2013*] and the derivation of V_P from a sine fit of the phonon dispersion. Combining the measured V_P with the bulk modulus derived from the equation of state, V_S can be determined as well, while the density is directly obtained from the collected diffraction patterns. In this study, we aim to establish precise relations between velocities (both V_P and V_S) and density for Fe and a representative Fe-Si alloy with 9 wt.% Si over a wide pressure range at room temperature. The results will provide a benchmark for calculations and will serve as reference for further studies of increased compositional complexity or addressing the temperature effects on the velocities.

2. Materials and Methods

Starting materials consisted in commercially available polycrystalline samples of Fe (99.998%, Alpha Aesar) and a Fe-Si alloy with 9 wt.% Si (Goodfellow, hereafter Fe-Si9). The same Fe-Si alloy was used in previous study of equation of state, with an average Si content measured by electron microprobe analysis of 8.87 wt% [*Zhang and Guyot, 1999*].

IXS and XRD measurements have been carried out at the European Synchrotron Radiation facility (ESRF) at ID28 and ID27 beamlines, respectively. IXS measurements have been performed on polycrystalline specimens compressed in a diamond anvil cell (DAC) using the Si(9,9,9) instrument configuration, which yields an overall energy resolution of 3 meV full width half maximum (FWHM). Absolute energies have been calibrated prior to the experiment comparing IXS diamond phonon dispersion with that obtained by inelastic neutron and Raman scattering. Specific to this experiment, we double-checked the energy calibration by comparing the sound velocity measured by IXS on iron powders at ambient conditions with the Voigt−Reuss−Hill average of ultrasonic determination on single crystal [*Guinan and Beshers, 1968*]. We also calibrated the scattering angle at the small working values of our IXS measurements by collection of diffraction from a silver behenate standard. Optics in Kirkpatrick-Baez configuration allowed focusing the x-ray beam at sample position at 30x70 μm^2 (horizontal x vertical, FWHM) or down to 12x7 μm^2 (horizontal x vertical, FWHM) depending upon DAC configuration. Momentum resolution was set by slits in front of the analyzers to 0.28 nm^{-1} and to 0.84 nm^{-1}, in the scattering plane and perpendicular to it. A vacuum chamber was used to minimize the quasi-elastic scattering contribution from air. Good-statistic data have been obtained with typical integration time of ~300 s per point for Fe, and ~500-600 s per point for Fe-Si9.

Pressures were generated by symmetric type, MAO DAC, using composite Re/c-BN gaskets, with either 150/300 μm beveled anvils, or 40/100/250 μm beveled anvils prepared by focus ion beam (FIB) milling technique [*Fei et al., 2016*]. Diamonds were pre-aligned and oriented to select the fastest transverse acoustic phonon of the diamond in the scattering plane and to minimize its intensity. The focused beam of 12x7 μm^2 FWHM at sample position granted collection of clean spectra on specimens down to ~35 μm in diameter. Such a small beam also permitted to probe phonons across moderate pressure gradients (as determined

105 from the fine diffraction mesh, see below), while the composite gasket ensured relatively
106 thick samples (8 to 12 μm at the highest pressure), and hence proper IXS signal, averaged
107 over a reasonably large number of grains. Pressure was increased off line by monitoring the
108 Raman spectra at the tip of the diamonds, and more precisely measured by the x-ray
109 diffraction according to known samples equation of state. Specifically we used a third-order
110 Birch-Murnaghan formalism, with V_0 = 22.47 Å^3/unit cell [*Dewaele et al. 2006*], K_0 = 155
111 GPa and K'= 5.37 [*Sakai et al., 2014*] for hcp-Fe and V_0 = 23.50 Å^3/unit cell, K_0 = 129 GPa
112 and K'= 5.24 for hcp-Fe-Si9 [*Fei, 2017*].

113 At each investigated pressure point, we mapped the aggregate longitudinal acoustic
114 phonon dispersion throughout the entire first Brillouin zone collecting 6 to 9 spectra in the 3-
115 12.5 nm^{-1} range. The energy positions of the phonons were extracted by fitting a set of
116 Lorentzian functions convolved with the experimental resolution function to the IXS spectra.
117 Figure 1 shows an example of the collected IXS spectra and the fitted result. We derived V_P
118 from a sine fit to the phonon dispersion [*Antonangeli et al., 2004*] (Figure 1), with error bars
119 between ±1 and ±3% for Fe and between ±2 and ±4% for Fe-Si9. The errors account for
120 statistical errors, finite energy and momentum resolution, as well as deviation from ideal
121 random orientation of the polycrystalline samples. Combining the measured V_P with bulk
122 modulus from the equation of state (the difference between isothermal and adiabatic bulk
123 modulus at 300 K is negligible), we also derived V_S [*Antonangeli et al., 2004*], with
124 uncertainties, obtained by propagating uncertainties on V_P and on K (the contribution from
125 uncertainties on density was observed to be negligible), between ±5 and ±6% for pure-Fe, and
126 between ±8 and ±10% for Fe-Si9 (assuming different equation of state leads to small effects
127 on V_S well within reported error bars).

128 For both samples, we collected angle dispersive 2D diffraction patterns at each
129 investigated pressure point, with a monochromatic wavelength of 0.3738Å (iodine K edge).

130 This allowed for clear structure determination and direct measurements of samples' density.
131 Taking advantage of the 3x3 μm^2 beam, we mapped the entire sample area, monitoring
132 pressure gradients across the sample chamber. Diffraction data are also used to detect any
133 developed texture. Examples of collected diffraction patterns are shown in Figure 2 and
134 Figure 3. The diffraction patterns of the compressed hcp-Fe (Figure 2) show rather smooth
135 rings, indicating the small sizes of the diffracting crystallites (average size ~25 nm at 167
136 GPa) and the good orientation averaging (only 100 reflection shows some variation in
137 intensity with the azimuthal angle). Two-dimensional detector images caked into rectilinear
138 projection show negligible dependence of the d spacing on the azimuthal angle around $2\theta=0$
139 direction (Figure 2), and hence a negligible deviatoric stress [*Wenk et al., 2006*]. Furthermore,
140 the (002) reflection, although weak, is still visible up to the highest attained pressure, further
141 highlighting the marginal preferential orientation. Such observations support the overall
142 validity of the random orientation approximation, critical to the analysis and interpretation of
143 the IXS results [*Antonangeli et al., 2004; Bosak et al., 2007;2016*]. The diffraction patterns
144 collected for the Fe-Si9 alloy (Figure 3) are somewhat less favorable than those on pure Fe, in
145 particular in term of sizes of crystallites (average size ~40 nm at 117 GPa) and randomness of
146 the distribution (intensity variation are quite visible for both 100 and 101 reflections), but they
147 are still acceptable. The (002) reflection, still visible at all probed pressure, is very weak, as a
148 direct consequence of a small preferential orientation fully developed already at 59 GPa and
149 not significantly evolving with pressure, with the c-axis preferentially aligned along the main
150 compression axis of the cell. Similar texture has been already reported in previous
151 experiments on iron [*Wenk et al., 2000*] and other metals with hcp structure [*Merkel et al.,*
152 *2006*]. Such a moderately increased deviation from the ideal random distribution is reflected
153 into the fairly increased error bars on the velocities derived from the IXS data (deviation from
154 ideal average can affect velocities up to 2%).

155 At the highest compression the maximum observed difference in pressure across the
156 sample chamber (~35 μm) is <7 GPa for Fe and <10 GPa for Fe-Si9. Over the volume seen by
157 IXS we obtain an average pressure of 167 GPa (Fe), with a standard deviation of 2 GPa and a
158 standard error of 1 GPa, and an average pressure of 144 GPa (Fe-Si9), with a standard
159 deviation of 2 GPa and a standard error of 1 GPa.

160

161 **3. Results**

162 The experimentally determined densities and velocities for hcp-Fe and hcp-Fe-Si9 are
163 summarized in Table 1. The details are presented below.

164 The measured compressional and shear sound velocities as a function of density for
165 hcp-Fe are plotted in Figure 4. These new measurements of V_P are in very good agreement
166 with the V_P-ρ linear relationship recently proposed by fitting combined datasets derived from
167 multiple techniques [*Antonangeli and Ohtani, 2015*], extending the data coverage at extreme
168 pressures. We notice that the extrapolation of the established trend to higher density is in
169 remarkable agreement with ab initio calculations at 0 K [*Vočadlo et al., 2009; Sha and Cohen,*
170 *2010*], clearly supporting a linear dependence of V_P on density. The derived V_S-ρ linear
171 relationship is also in general agreement with results of ab initio calculations at 0 K. We also
172 noticed the good agreement between the slope of our V_S-ρ trend with that obtained by the
173 most recent nuclear resonant inelastic x-ray scattering (NRIXS) experiments [*Murphy et al.,*
174 *2013; Gleason et al., 2013; Liu et al., 2016*], even if actual V_S values derived by NRIXS are
175 somewhat lower, between 3 to 8% depending upon datasets. Such a difference is at least
176 partially due to the enrichment in heavier Fe isotopes of samples used for NRIXS studies with
177 respect to sample of natural isotopic abundance used here.

178 The measured compressional and shear sound velocities as a function of density for
179 hcp-Fe-Si9 are shown in Figure 5. Our V_P measurements on samples with 9 wt.% Si are very
180 close to previous IXS measurements on samples with 8 wt.% Si [*Mao et al., 2012*], but they
181 are systematically higher than early determination by NRIXS on samples with 8 wt.% Si [*Lin*
182 *et al., 2003*]. Similar to the case of pure Fe, our measurements support a linear dependence of
183 V_P on ρ for Fe-Si9. The derived V_S-ρ relationship can be well described by a second order
184 polynomial (Figure 5).

185 Comparison of results obtained for Fe and Fe-Si9 (Figure 6) show that Si alloying
186 systematically increases V_P at constant density over the investigated pressure range. Linear
187 fits indicate that, even if V_P of the Fe-Si9 alloy increases with density slower than pure Fe,
188 Fe-Si9 is still expected to have significantly higher V_P than Fe at inner core density (~12390
189 m/s vs. ~11680 m/s at 13000 kg/m^3). On the other hand, the derived density evolution for V_S
190 of Fe-Si9 is such that the Si-bearing alloys is expected to have higher V_S than pure Fe only up
191 to ρ≈11200 kg/m^3, with V_S of Fe larger than V_S of Fe-Si9 at inner core density (~5130 m/s vs.
192 ~5890 m/s at 13000 kg/m^3). This trend (i.e V_P increasing with Si content and V_S decreasing)
193 has been reported as well by recent ab initio calculations of Fe-Si alloys at core pressures
194 [*Martorell et al., 2016*]. However, on the contrary to the case of pure Fe, the extrapolation of
195 our experimental results for Fe-Si9 does not agree with the calculations.

196

197 **4. Discussion**

198 Concerning hcp-Fe, we note a remarkable agreement between our new measurements,
199 previous measurements by various techniques and ab initio calculations for V_P, and a
200 reasonable agreement for V_S. The established consensus provides very strong constraints on
201 the linear dependence of velocities on density and on actual values of velocities of hcp-Fe at

inner core densities and 300 K (Figure 4), which can by now be considered known within few percent (with V_P better constrained than V_S).

Somewhat less evident is the case for Si bearing hcp Fe-alloys. Literature data obtained in the ~40 to ~100 GPa range on samples of the same nominal composition [*Lin et al., 2003; Mao et al., 2012*] are in clear disagreement (Figure 5). Reasons for the discrepancy between NRIXS [*Lin et al., 2003*] and IXS [*Mao et al., 2012*] data possibly include systematic differences due to the techniques, or due to the sample's texture. The V_P measured in this study are in a good agreement with previous IXS determination at lower pressures [*Mao et al., 2012*] and significantly extend the probed pressure range. In view of our new data, a sub-linear relationship between V_P and density, as proposed by *Mao et al., [2012]* on the basis of data over a more restricted pressure range, seems not justified. Linear extrapolation of experimental results to inner core density and comparison with calculations [*Tsuchiya and Fujibuki, 2009; Martorell et al., 2016*] show however a disagreement, more important for V_P than for V_S. The difference would be even more striking when considering a power-law sub-linear extrapolation. In particular, the calculations seem to overestimate the effect of Si on V_P of the Fe-Si alloys. We noticed that ab initio calculations on Fe-Si alloys, even when performed at 0 K, give quite conflicting results [*Tsuchiya and Fujibuki, 2009; Martorell et al., 2016*], highlighting the difficulty in performing calculations taking into account the configurational order/disorder inherent to alloys. Further investigation by both experiments and theoretical calculations is necessary to resolve the discrepancy.

The direct comparison between results obtained on Fe and on Fe-Si9 allows us to address the effect of Si content on the velocities of a hcp $Fe_{1-x}Si_x$ alloy in the limit of low to moderate Si concentration (0 to 9wt.%). The simplest approach is to use an ideal linear mixing model [e.g. *Badro et al., 2007; Antonangeli et al., 2010*]. Using the reference relations established here for pure Fe and the extrapolation of our measurements on Fe-Si9, at the inner

core density of 13000 kg/m^3 we get a variation ~ +80 m/s on V_P and ~ -80 m/s on V_S for each wt.% of Si (Figure 6). Measurements of V_P on an Fe-Ni-Si alloy with 4.3wt.% Ni and 3.7wt.% Si [*Antonangeli et al., 2010*] extrapolated to 13000 kg/m^3 yield V_P~12100 m/s, in good agreement with our estimate of V_P~11980 m/s for a Fe-Si alloy with 3.7wt.%Si (difference ~ -1%). This agreement argues in favor of the suitability of the here-proposed estimate. Moreover it suggests that the effect on the compressional sound velocity due to Ni inclusion at level of 4 to 5 wt.% is minor. Further independent support also comes from the good agreement observed between our predicted value of V_P~12160 m/s and the extrapolation of very new measurements on a Fe-Si alloy with 6wt.% Si [*Sakairi et al., Am. Min. in press.*] yielding V_P~11940 m/s (difference ~ +1.8%).

In order to use our data to assess the Si abundance in the inner core by comparison with seismological models, the effects of high temperature have to be accounted for. A velocity vs. density representation, as the one proposed here, implicitly accounts for quasi-harmonic effects, but anharmonic effects might be important as well, in particular on V_S and for temperatures approaching melting. Sound velocity measurements at simultaneous high pressure and high temperature conditions are at the cutting edge of current technical capabilities and only few datasets are available, mostly for pure Fe [e.g. *Antonangeli et al., 2012; Mao et al., 2012; Ohtani et al., 2013; Sakamaki et al., 2015*]. If we model high-temperature effects for Fe following *Sakamaki et al. [2015]*, V_P is expected to be lowered by ~ -0.09 m/s K^{-1} at the constant density of 13000 kg/m^3. The orange arrow in Figure 4 highlights the magnitude of the expected reduction of V_P for T up to ~7000 K. Alternatively we can model temperature-induced softening (in this case for both V_P and V_S) following calculations by *Martorell et al., [2013]*. As these calculations have been performed at constant pressure, while here we are interested in the effects at constant density, we corrected the computed values according to the measured density dependence of sound velocities to

compensate for the effects due to density variation with increasing temperature. Once limiting to T up to 7000 K, the estimated lowering of V_P and V_S are, respectively, ~ -0.12 m/s K^{-1} and ~ -0.32 m/s K^{-1} at the constant density of 13000 kg/m^3. The violet arrows in Figure 4 highlights the magnitude of the expected reduction of V_P and V_S for T up to ~7000 K. In qualitative agreement with recent calculations, for Fe, temperature effects alone permit to match inner core velocities (but not densities, which remain too high for pressures in the range 330 to 360 GPa). In the case of Fe-Si alloys we can only rely on calculations [*Martorell et al., 2016*], which, once corrected as in the case of Fe, yield for a sample with 3.2 wt% Si a reduction of V_P and V_S of, respectively, ~ -0.12 m/s K^{-1} and ~ -0.34 m/s K^{-1}, and for a sample with 6.7 wt% Si a reduction of ~ -0.20 m/s K^{-1} and ~ -0.23 m/s K^{-1}, at the constant density of 13000 kg/m^3. We note that theoretical estimates for pure Fe and a Fe-Si alloy with 3.2wt.% Si are very close, while those for a Fe-Si with 6.7wt.% Si differ, with an effect on V_P almost double and an effect on V_S about 30% smaller. The arrows in Figure 5 highlights the magnitude of the expected reduction of V_P and V_S for T up to ~7000 K if we apply to our measurements on Fe-Si9 the correction estimated for samples with 3.2wt.% Si (dark blue arrows) or that for samples with 6.7 wt.% Si (green arrows). Similarly to the case of Fe, if temperature effects are as large as expected according to calculations, temperature alone might be enough to explain inner core velocities (but again, not the densities, too low for pressures in the 330 to 360 GPa range for samples with 9 wt.% Si [*Tateno et al., 2015*]).

If we assume temperature effects at the constant density of 13000 kg/m^3 of ~ -0.20 m/s K^{-1} for V_P and ~ -0.23 m/s K^{-1} for V_S (as from estimates from calculations on a sample with 6.7 wt% Si) we match PREM values of V_P and V_S for a Si concentration of 10±1 wt.% and T between 6500 and 6700 K. This solution however is not acceptable, as such Fe-Si alloy is expected to have the right density only for pressures well above 360 GPa [*Tateno et al., 2015*]. If we assume temperature effects at the constant density of 13000 kg/m^3 of ~ -0.12 m/s K^{-1} for

V_P and ~ -0.33 m/s K^{-1} for V_S (as from estimates from calculations on pure Fe and on a sample with 3.2 wt% Si) we obtain PREM values of V_P and V_S for a Si concentration of 3±2 wt.% and T between 6200 and 6500 K. P-V-T relation for a Fe-Si alloy with ~3 wt.% Si has not been experimentally determined yet, but calculations suggest such an alloy to have a density of ~13160 kg/m^3 at 360 GPa and 6400 K [*Martorell et al., 2016*], thus making this solution acceptable. Furthermore, an inner core temperature of 6200-6500 K is compatible with estimates based on measurements of the Fe and Fe-Si alloys melting curve [*Anzellini et al., 2013; Morard et al., 2011*]. However, as already mentioned, the most recent experimental determination of temperature dependence of V_P for Fe by *Sakamaki et al. [2016]* argues for a less important temperature-induced lowering with respect to that proposed by calculations. If we assume temperature effects at the constant density of 13000 kg/m^3 of ~ -0.09 m/s K^{-1} for V_P as from *Sakamaki et al. [2016]*, we match PREM value of V_P for ~1 wt.% Si at 6300 K and ~2 wt.% Si at 7300 K. The last solution is not acceptable as a Fe-Si alloy is not solid at such a high temperatures [*Morard et al., 2011; Anzellini et al., 2013*]. Furthermore, irrespectively whether we assume a temperature effect on V_S of ~ -0.33 m/s K^{-1} (as from estimates from calculations on pure Fe and a Fe-Si alloy with 3.2 wt.% Si), or ~ -0.23 m/s K^{-1} (as from estimates from calculations on Fe-Si alloy with 6,7 wt.% Si), or ~ -0.24 m/s K^{-1} for V_S (scaling the estimates from calculations on pure Fe in line with the reduced effect on V_P), there is no solution matching PREM values of V_P and V_S for a fixed Si content. Further constraints on the effects of high-temperature on sound velocities thus remain crucial to reliably estimate the Si content in the inner core.

5. Conclusions

We carried out sound velocity and density measurements on solid hcp-Fe and an hcp-Fe-Si alloy with 9 wt.% Si up to ~170 and ~ 140 GPa, respectively. The experimentally

established V_P-ρ and V_S-ρ relations for pure Fe are in good agreement with results from ab initio calculations and clearly show that both compressional and shear velocities scale linearly with density at 300 K (Figure 4). At 300 K and the inner core density of 13000 kg/m^3, the reference values for V_P and V_S are respectively 11680±250 m/s and 5890±360 m/s. Measurements on the Fe-Si alloy with 9 wt.% Si allowed us to discriminate between previous inconsistent datasets (Figure 5) and to propose V_P-ρ and V_S-ρ relations for Fe-Si9. These results are used to address the presence and abundance of Si in the Earth's inner core.

From a methodological standpoint, constraints coming only from density [e.g. *Tateno et al., 2015*] or even by combined density and compressional sound velocity [e.g. *Badro et al., 2007; Mao et al., 2012; Ohtani et al., 2013*] can be used to exclude possibilities, but it is necessary to simultaneously consider V_P, V_S and ρ to propose a consistent composition for the Earth's inner core. Qualitatively, at inner core conditions, high temperature reduces sound velocities, even at constant density, while Si alloying at level of 9 wt.%, lowers ρ, increases V_P and decreases V_S with respect to pure Fe. These same effects have been very recently suggested by calculations on Fe-Si alloys [*Martorell et al., 2016*], as well as for carbon alloys [*Caracas, 2017*]. Assuming an ideal linear mixing model to be valid for low to moderate Si concentration (<10wt.%), we quantitatively evaluate the effect in ~ +80 m/s on V_P and ~ -80 m/s on V_S for each wt.% of Si at the inner core density of 13000 kg/m^3. Further studies on samples of intermediate compositions will allow refinement of this estimation.

We explored the possible solutions for an hcp-Fe-Si alloy whose density, compressional and shear sound velocities would match PREM values for pressures in the range 330 to 360 GPa and temperatures in the range 4000 to 7500 K. The existence of a solution and the amount of Si necessary to match the seismological observations strongly depends on the way we model anharmonic effects on sound velocities at high temperature and on core temperature. In particular, we obtain possible solutions only for large temperature corrections, relatively

high core temperatures (with T comprised between 6200 and 6500 K), and for Si content not exceeding 3±2 wt.% Si. Accordingly, the current results do not support the presence of Si in the inner core at a level of 6 to 8 wt.% as recently proposed [*Mao et al., 2012; Fischer et al., 2015; Tateno et al., 2015*]. On the sole basis of density and sound velocities systematics, we cannot discriminate between results proposing little (up to 4 wt.%) [e.g. *Badro et al., 2007; Antonangeli et al., 2010*] to no presence [*Martorell et al., 2016*] of Si in the inner core. More experimental and theoretical work on Fe-Si alloys remains to be performed, so as to extend the directly probed pressure and temperature range and to check the limit of the ideal mixing approximation. We also encourage performing calculations not only at actual core conditions, but as well at conditions where experimental data exist, so as to validate theoretical treatments of alloys.

Acknowledgments

This work was supported by the Investissements d'Avenir programme (reference ANR-11-IDEX-0004-02) and more specifically within the framework of the Cluster of Excellence MATériaux Interfaces Surfaces Environnement (MATISSE) led by Sorbonne Universités (grant to DA). The research was also supported by the Carnegie Institution for Science and NSF (grant EAR-1619868 to YF). Authors wish to thank Sébastien Merkel for discussion about texture and preferential orientations.

References

Antonangeli, D., F. Occelli, H. Requardt, J. Badro, G. Fiquet, M. Krisch (2004), Elastic anisotropy in textured hcp-iron to 112 GPa from sound wave propagation measurements, *Earth Planet. Sci. Lett. 225*, 243–251.

Antonangeli, D., J. Siebert, J. Badro, D.L. Farber, G. Fiquet, G. Morard, F.J. Ryerson (2010), Composition of the Earth's inner core from high-pressure sound velocity measurements in Fe–Ni–Si alloys, *Earth Planet. Sci. Lett. 295*, 292–296.

Antonangeli, D., T. Komabayashi, F. Occelli, E. Borissenko, A.C. Walters, G. Fiquet, Y. Fei, (2012), Simultaneous sound velocity and density measurements of hcp iron up to 93 GPa and 1100 K: An experimental test of the Birch's law at high temperature, *Earth Planet. Sci. Lett. 331-332*, 210–214.

Antonangeli, D., and E. Ohtani (2015), Sound velocity of hcp-Fe at high pressure: experimental constraints, extrapolations and comparison with seismic models, *Prog. Earth Planet. Sci. 2*, 3.

Antonangeli, D., G. Morard, N.C. Schmerr, T. Komabayashi, M. Krisch, G. Fiquet, Y. Fei (2015), Toward a mineral physics reference model for the Moon's core, *Proc. Natl. Acad. Sci. USA 112*, 3916–3919.

Anzellini, S., A. Dewaele, M. Mezouar, P. Loubeyre, G. Morard (2013), Melting of iron at Earth's inner core boundary based on fast x-ray diffraction, *Science 340*, 464–466.

Badro, J., G. Fiquet, F. Guyot, E. Gregoryanz, F. Occelli, D. Antonangeli, M. d'Astuto (2007), Effect of light elements on the sound velocities in solid iron: implications for the composition of Earth's core, *Earth Planet. Sci. Lett. 254*, 233–238.

Birch, F. (1952). Elasticity and constitution of the Earth's interior, J. *Geophys. Res. 57*, 227–286.

Bosak, A., M. Krisch, I. Fischer, S. Huotari, G. Monaco (2007), Inelastic x-ray scattering from polycrystalline materials at low momentum transfer, *Phys. Rev. B 75*, 064106.

373 Bosak, A., M. Krisch, A. Chumakov, I.A. Abrisokov, L. Dubrovinsky (2016), Possible
374 artifacts in inferring seismic properties from X-ray data, *Phys. Earth Planet. Inter.260*,
375 14–19.

376 Caracas., R. (2017). The influence of carbon on the seismic properties of solid iron, *Geophys.*
377 *Res. Lett. 44*, 128–134.

378 Crowhurst, J.C., A.F. Goncharov, J.M. Zaug (2004), Impulsive stimulated light scattering
379 from opaque materials at high pressure, *J. Phys. Condens. Matter. 16*, S1137–S1142.

380 Decremps, F., D. Antonangeli, M. Gauthier, S. Ayrinhac, M. Morand, G. Le Marchand, F.
381 Bergame, J. Philippe (2014), Sound velocity measurements of iron up to 152 GPa by
382 picosecond acoustics in diamond anvil cell, *Geophys. Res. Lett. 41*, 1459.

383 Dziewonski, A.M., and D.L. Anderson (1981). Preliminary reference Earth model, P*hys.*
384 *Earth Planet. Inter. 25*, 297–356.

385 Fiquet, G., J. Badro, F. Guyot, H. Requardt, M. Krisch (2001). Sound velocities in iron to 110
386 gigapascals, *Science 291*, 468–471.

387 Fiquet, G., J. Badro, E. Gregoryanz, Y. Fei, F. Occelli (2009). Sound velocity in iron carbide
388 (Fe_3C) at high pressure: Implications for the carbon content of the Earth's inner core,
389 *Phys. Earth Planet. Inter. 172*, 125–129.

390 Fischer, R.A., Y. Nakajima, A.J. Campbell, D.J. Frost, D. Harries, F. Langenhorst, N.
391 Miyajima, K. Pollok, D.C. Rubie (2015), High pressure metal–silicate partitioning of Ni,
392 Co, V, Cr, Si, and O, *Geochim. Cosmochim. Acta 167*, 177–194.

393 Fei, Y. (2017). Unpublished data.

394 Fei, Y., C. Murphy, Y. Shibazaki, A. Shahar, and H. Huang (2016), Thermal equation of state
395 of hcp-iron: Constraint on the density deficit of Earth's solid inner core, *Geophys. Res.*
396 *Lett. 43*, 6837–6843.

397 Gleason, A.E., W.L. Mao, J.Y. Zhao (2013), Sound velocities for hexagonally closepacked
398 iron compressed hydrostatically to 136 GPa from phonon density of states, *Geophys.*
399 *Res. Lett. 40*, 2983–2987.

400 Guinan, M.W., and D.N. Beshers (1968), Pressure derivatives of the elastic constants of α-
401 iron to 110 kbs, *J. Phys. Chem. Solids 29*, 541–549.

402 Lin, J.-F., V.V. Struzhkin, W. Sturhahn, E. Huang, J. Zhao, Y.H. Hu, E.E. Alp, H.-K. Mao, N.
403 Boctor, J. Hemley (2003), Sound velocities of iron–nickel and iron–silicon alloys at
404 high pressures. *Geophys. Res. Lett. 30*, 2112.

405 Liu, J., J.-F. Lin, A. Alatas, A., M.Y. Hu, J. Zhao, L. Dubrovinsky (2016), Seismic parameters
406 of hcp-Fe alloyed with Ni and Si in the Earth's inner core, *J. Geophys. Res. Solid Earth*
407 *121*, 610–623.

408 Mao, H.K, Y. Wu, L.C. Chen, J.F. Shu, A.P. Jephcoat (1990), Static compression of iron to
409 300 GPa and $Fe_{0.8}Ni_{0.2}$ alloy to 260 GPa: Implications for composition of the core, *J.*
410 *Geophys. Res. 95*, 21737-21742.

411 Mao, H.K., J. Shu, G. Shen, R.J. Hemley, B. Li, A.K. Singh (1998), Elasticity and rheology
412 of iron above 220 GPa and the nature of the Earth's inner core. *Nature 396*, 741–743;
413 correction (1999) *Nature 399*, 80.

414 Mao, Z., J.-F. Lin, J. Liu, A. Alatas, L. Gao, J. Zhao, H.-K. Mao (2012), Sound velocities of
415 Fe and Fe–Si alloy in the Earth's core, *Proc. Natl. Acad. Sci. USA 109*, 10239–10244.

416 Martorell, B., L. Vočadlo, J. Brodholt, I.G. Wood (2013), Strong pre-melting effect in the
417 elastic properties of hcp-Fe under inner-core conditions, *Science 342*, 466–468.

418 Martorell, B., I.G. Wood, J., Brodholt, L. Vočadlo (2016), The elastic properties of hcp-
419 $Fe_{1-x}Si_x$ at Earth's inner-core conditions, *Earth Planet. Sci. Lett. 451*, 89–96.

420 Merkel, S., N. Miyajima, D. Antonangeli, G. Fiquet, T. Yagi (2006). Lattice preferred
421 orientation and stress in polycrystalline hcp-Co plastically deformed under high
422 pressure, *J. Appl. Phys. 100*, 023510.

423 Morard, G., D. Andrault. N. Guignot, J. Siebert, G. Garbarino, D. Antonangeli (2011),
424 Melting of Fe-Ni-Si and Fe-Ni-S alloys at megabar pressures: implications for the core-
425 mantle boundary temperature, *Phys. Chem. Minerals 38*, 767–776.

426 Murphy, C.A., J.M. Jackson, W. Sturhahn (2013), Experimental constraints on the
427 thermodynamics and sound velocities of hcp-Fe to core pressures, *J. Geophys. Res.*
428 *Solid Earth 118*, 1–18.

429 Ohtani, E., Y. Shibazaki, T. Sakai, K. Mibe, H. Fukui, S. Kamada, T. Sakamaki, Y. Seto, S.
430 Tsutsui, A.Q.R. Baron (2013), Sound velocity of hexagonal close-packed iron up to
431 core pressures, *Geophys. Res. Lett. 40*, 5089–5094.

432 Prescher, C., and V.B. Prakapenka (2015), DIOPTAS: a program for reduction of two-
433 dimensional X-ray diffraction data and data exploration, *High Pressure Research 35*,
434 223–230.

435 Sakai, T., S. Takahashi, N. Nishitani, I. Mashini, E. Ohtani, N. Hirao (2014), Equation of state
436 of pure iron and Fe0.9Ni0.1 alloy up to 3 Mbar, *Phys. Earth Planet. Inter. 228*, 114–126.

437 Sakairi, T., T. Sakamaki, E. Ohtani, H. Fukui, S. Kamada, S. Tsutsui, H. Uchiyama, A.Q.R.
438 Baron (2017), *American Mineralogist, in press. DOI: http://dx.doi.org/10.2138/am-*
439 *2018-6072.*

440 Sakamaki, T., E. Ohtani, H. Fukui, S. Kamada, S. Takahashi, T. Sakairi, A. Takahata, T.
441 Sakai, S. Tsutsui, D. Ishikawa, R. Shiraishi, Y. Seto, T. Tsuchiya, A.Q.R. Baron (2016),

442 Constraints on Earth's inner core composition inferred from measurements of the sound
443 velocity of hcp-iron in extreme conditions, *Sci. Adv. 2*, e1500802.

444 Sha, X., and R.E. Cohen (2010), Elastic isotropy of ε-Fe under Earth's core conditions,
445 *Geophys. Res. Lett. 37*, L10302.

446 Siebert, J., J. Badro, D. Antonangeli, F.J. Ryerson (2013), Terrestrial accretion under
447 oxidizing conditions, *Science 339*, 1194–1197.

448 Tateno, S., K. Hirose, Y. Ohishi, Y. Tatsumi (2010), The structure of iron in the Earth's core,
449 *Science 330*, 359–361.

450 Tateno, S., Y. Kuwayama, K. Hirose, Y. Ohishi (2015), The structure of Fe-Si alloy in the
451 Earth's inner core, *Earth Planet. Sci. Lett. 418*, 11–19.

452 Tsuchiya, T., and M. Fujibuki (2009), Effects of Si on the elastic property of Fe at Earth's
453 inner core pressures: Frist principles study, *Phys. Earth Planet. Inter. 174*, 212–219.

454 Vočadlo, L., D. Dobson, I.G. Wood (2009), Ab initio calculations of the elasticity of hcp-Fe
455 as a function of temperature at inner-core pressure, *Earth Planet. Sci. Lett. 288*, 534–
456 538.

457 Wenk, H.R., S. Matthies, R.J. Hemley, H.-K. Mao, J. Shu (2000), The plastic deformation of
458 iron at pressures of the Earth's inner core, *Nature 405*, 1044–1047.

459 Wenk, H.R., I. Lonardelli, S. Merkel, L. Miyagi, J. Pehl, S. Speziale, C.E. Tommaseo (2006),
460 Deformation textures produced in diamond anvil experiments, analyzed in radial
461 diffraction geometry, *J. Phys.: Cond. Matter 18*, S933–S947.

462 Zhang, J. and F. Guyot (1999), Thermal equation of state of iron and $Fe_{0.91}Si_{0.09}$, *Phys. Chem.*
463 *Miner. 26*, 206–211.

464

Figures

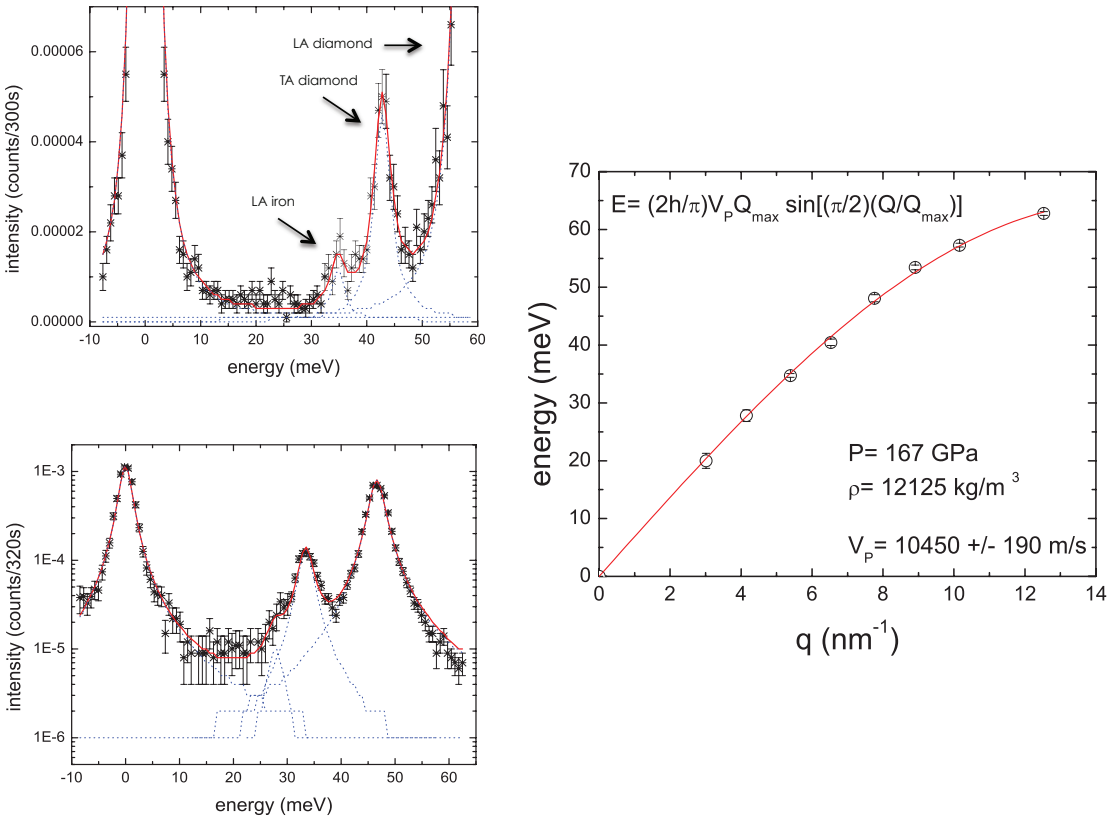

Figure 1. Examples of IXS spectra (left) and aggregate phonon dispersion (right) obtained for pure-Fe at the highest investigated pressure (ρ=12125 kg/m^3, corresponding to ~167 GPa). Up left: IXS spectrum for q=5.39 nm^{-1}; bottom left IXS spectrum for q=4.15 nm^{-1}. IXS spectra are characterized by an elastic line, centered around zero, and inelastic features, assigned for increasing energy to the longitudinal acoustic (LA) aggregate phonon of iron and the transverse acoustic (TA) and longitudinal acoustic (LA) phonons of diamond. The experimental points and error bars are shown together with the best-fit (red line) and individual excitations (dashed blue lines). Sample phonons for q of 5.39 nm^{-1} and higher are well resolved and visible in linear scale, while for smaller q values, sample phonons and TA phonon of diamonds get very close, and sample phonons become a shoulder on the low-energy side of the TA phonon of diamond, better visible in logarithmic scale.

478

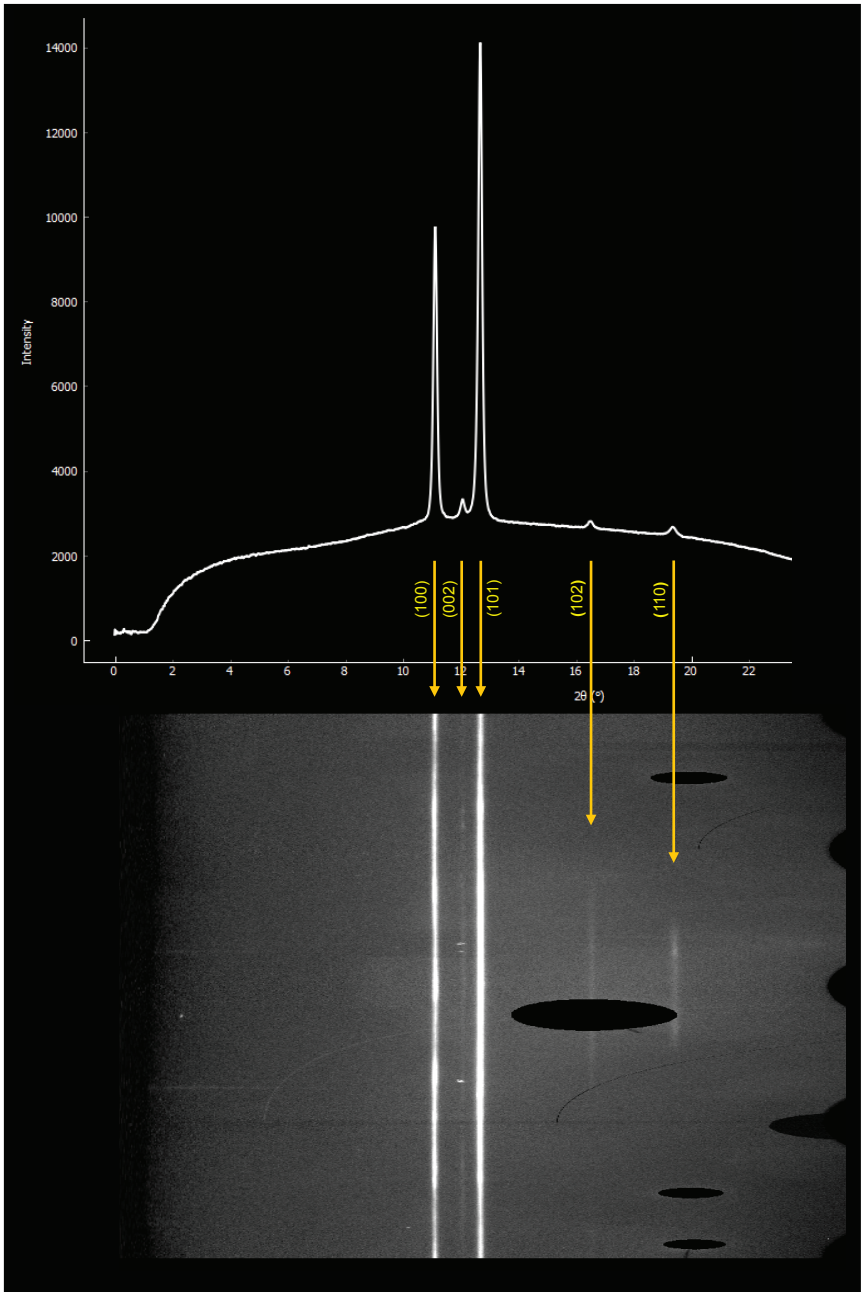

Figure 2. Example of integrated diffraction pattern collected on pure hcp-Fe at P~167 GPa (top) and caked into a rectilinear projection (bottom). 2D diffraction images have been integrated using Dioptas [Prescher and Prakapenka, 2015].

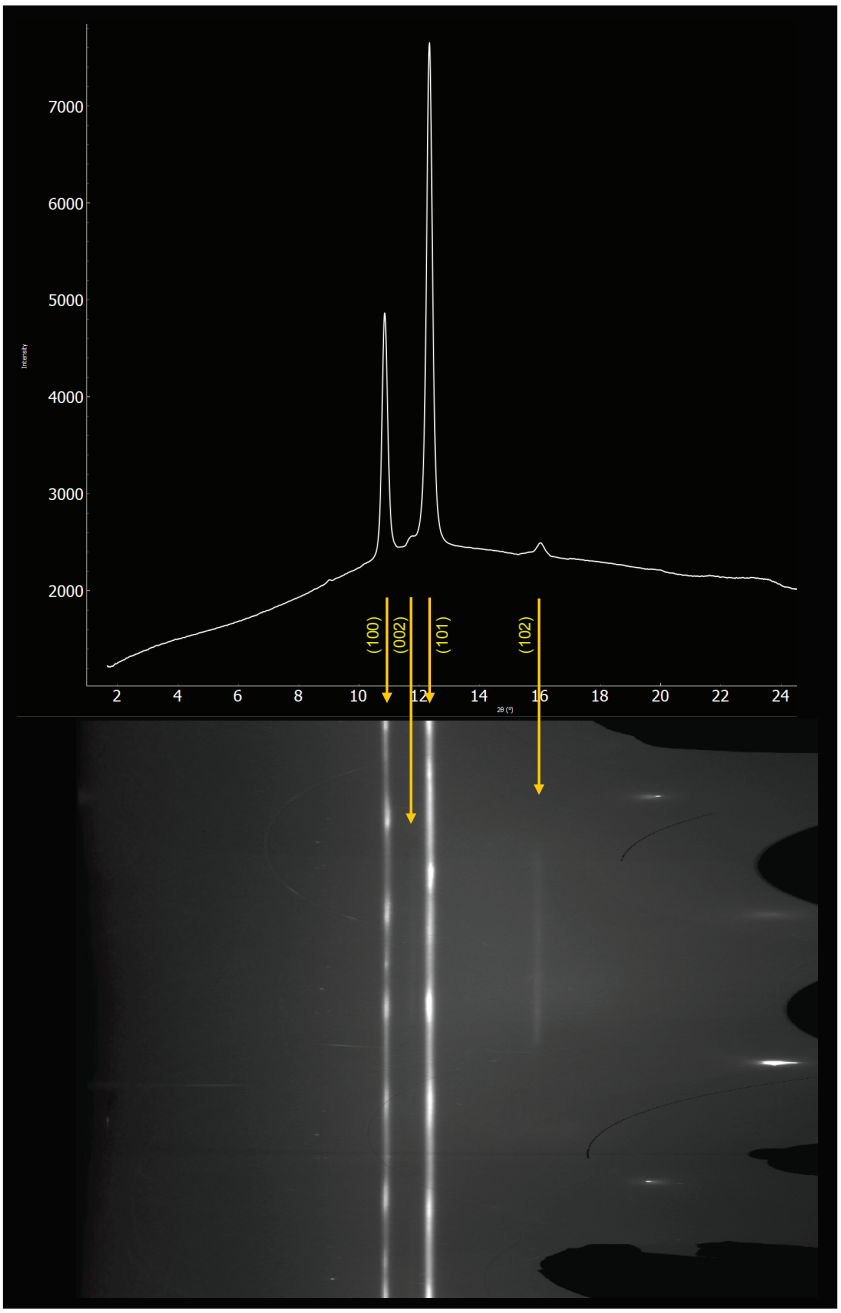

485

486

487 **Figure 3. Example of integrated diffraction pattern collected on hcp-FeSi9 at**

488 **P~117 GPa (top) and caked into a rectilinear projection (bottom)**. 2D diffraction images

489 have been integrated using Dioptas [Prescher and Prakapenka, 2015].

490

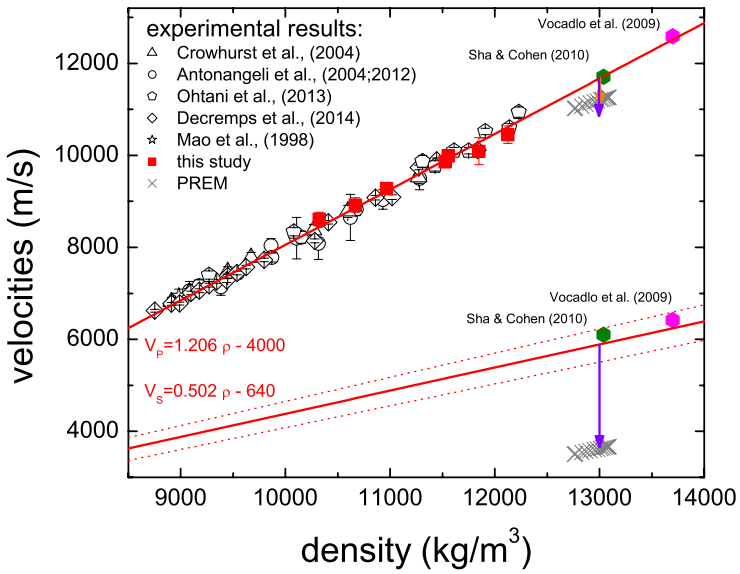

491

492

493 **Figure 4. Aggregate compressional (V_P) and shear (V_S) sound velocities of hcp-Fe**
494 **at 300 K as a function of density**. Results of this study are compared with a selection of
495 published measurements at 300 K [Mao et al., 1998; Crowhurst et al., 2004; Antonangeli et al.,
496 2004, 2012; Ohtani et al., 2013; Decremps et al., 2014] (for further details see Antonangeli
497 and Ohtani [2015]), ab initio calculations at 0 K and 295 GPa [Vočadlo et al., 2009] and at 0
498 K and 13040 kg/m^3 [Sha and Cohen, 2010]. PREM [Dziewonski and Anderson, 1981] is
499 reported as crosses. Solid lines show the established linear V_P-ρ and V_S-ρ relationships.
500 Dotted lines show confidence level on the derived V_S. Arrows indicate possible magnitude of
501 anharmonic effects up to 7000 K (see text).

502

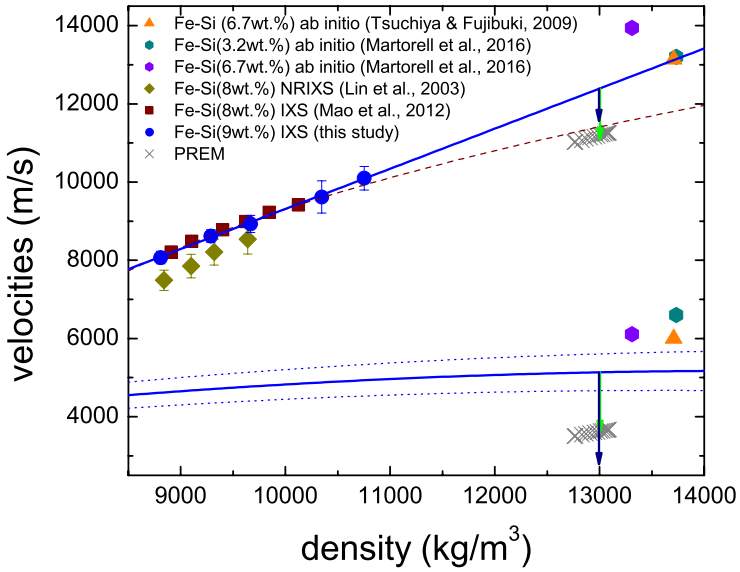

503

504

505 **Figure 5. Aggregate compressional (V_P) and shear (V_S) sound velocities of hcp-Fe-**
506 **Si9 at 300 K as a function of density**. Results of this study are compared with measurements
507 at 300 K on a hcp-Fe-Si alloy with 8 wt.% Si by NRIXS [Lin et al., 2003] and by IXS [Mao et
508 al., 2012] as well as with results of ab initio calculations at 0 K and 360 GPa on an hcp-Fe-Si
509 alloy with 6.7 wt.% Si [Tsuchiya and Fujibuki, 2009] and at 0 K and 360 GPa on hcp-Fe-Si
510 alloys with 3.2 and 6.7 wt.% Si [Martorell et al., 2016]. PREM [Dziewonski and Anderson,
511 1981] is reported as crosses. Solid lines show the proposed V_P-ρ (V_P=1.026×ρ-946) and V_S-ρ
512 (V_S=1530+0.503×ρ-1.736×10^{-5}×ρ^2) relationships. Dotted lines show confidence level on the
513 derived V_S. The dashed line is the empirical power-law function used by Mao et al., [2012] to
514 describe their V_P-ρ data. Arrows indicate possible magnitude of anharmonic effects up to
515 7000 K (see text).

516

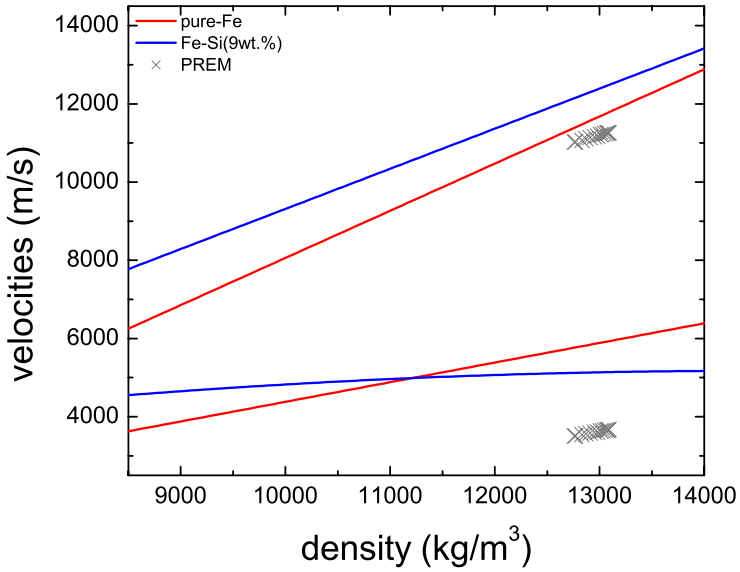

517

518

519 **Figure 6. Comparison of the proposed density dependence of the aggregate**

520 **compressional (V_P) and shear (V_S) sound velocities of hcp-Fe (red) and hcp-FeSi9 (blue)**

521 **extrapolated to core density, along with PREM [Dziewonski and Anderson, 1981] shown**

522 **as crosses.**

523 **Table 1. Measured densities and compressional sound velocities (V_P)**. Pressure
524 estimated from measured diffraction patterns are reported as well. See text for discussion of
525 pressure uncertainties and pressure gradients. Assuming different equation of state for hcp-Fe
526 leads to a maximum difference in the reported pressure of less than 10 GPa at the highest
527 density when using equation of state from Mao et al., [1990].

Sample	Density (kg/m^3)	Pressure (GPa)	V_P (m/s)
hcp-Fe	10325	63	8610±150
hcp-Fe	10665	79	8920±160
hcp-Fe	10965	96	9280±90
hcp-Fe	11525	124	9860±110
hcp-Fe	11555	126	9990±120
hcp-Fe	11850	146	10090±290
hcp-Fe	12125	167	10450±190
hcp-Fe-Si9[a]	8805	42	8070±170
hcp-Fe-Si9	9285	59	8620±160
hcp-Fe-Si9	9665	79	8930±220
hcp-Fe-Si9	10350	117	9620±410
hcp-Fe-Si9	10755	144	10100±300

528 [a] This point have been collected on decompression.